Available online at www.sciencedirect.com
ScienceDirect
Construction and Building Materials 21 (2007) 1311–1321
Construction and Building MATERIALS
www.elsevier.com/locate/conbuildmat

Ambient vibration testing of historic masonry towers for structural identification and damage assessment

C. Gentile *, A. Saisi

Department of Structural Engineering, Polytechnic of Milan, Piazza Leonardo da Vinci, 32 20133 Milan, Italy

Received 22 July 2005; received in revised form 10 January 2006; accepted 15 January 2006
Available online 17 October 2006

Abstract

The results of the ambient-vibration based investigations carried out to assess the structural conditions of a masonry bell-tower are presented. The tower, dating back to the XVII century and about 74 m high, is characterised by the presence of major cracks on the western and eastern load-bearing walls.

The assessment procedure includes full-scale ambient vibration testing, modal identification from ambient vibration responses, finite element modelling and dynamic-based identification of the uncertain structural parameters of the model. A good match between theoretical and experimental modal parameters was reached for relatively low stiffness ratios in the most damaged regions of the tower. Furthermore, the model identification, carried out by using two different methods, provided consistent structural parameters which are also in close agreement with the available characterization of the materials.

Keywords: Ambient vibration test; Damage; Operational modal analysis; F.e. model identification; Masonry towers

1. Introduction

In the last decade, the conservation and the structural safety assessment of ancient masonry towers have become of increasing concern, probably as a consequence of some dramatic events registered in Europe, like the sudden collapse of the Civic Tower in Pavia, Italy [1,2] and of the bell-tower of St. Magdalena in Goch, Germany. Examples of recent investigations include well-known towers, such as the "Torrazzo" in Cremona (the highest masonry tower in Europe, [3]), the Civic Tower in Vicenza [4], the St. Stefano bell-tower in Venice [5]; generally, these investigations involve both analytical and experimental analysis including several tasks: field survey of the "as built" configuration and of the crack pattern, non-destructive and slightly destructive tests (e.g. flat-jack tests or sonic pulse velocity tests), laboratory tests on cored samples, finite element modelling and theoretical analysis.

In the paper, an ambient vibration-based procedure has been applied to assess the structural condition and the damage scenario of the historic masonry bell-tower, adjacent to the Cathedral of Monza (a town about 20 km far from Milan, Italy). The dynamic-based assessment, involving both theoretical and experimental modal analysis, includes the following main steps (Fig. 1):

1. Ambient vibration testing.
2. Operational modal analysis (*OMA*), i.e. the extraction of modal parameters (natural frequencies and mode shapes) from output-only experimental data.
3. Finite element analysis (*FEA*) and correlation with the experimental results.
4. Identification of the uncertain structural parameters of the model (model updating) [6] by minimizing the difference between theoretical and experimental modal behaviour.

The dynamic tests were carried out to complement an extensive research program [7,8] planned to evaluate the structural condition of the tower, characterised by the pres-

* Corresponding author.

0950-0618/$ - see front matter © 2006 Elsevier Ltd. All rights reserved.
doi:10.1016/j.conbuildmat.2006.01.007

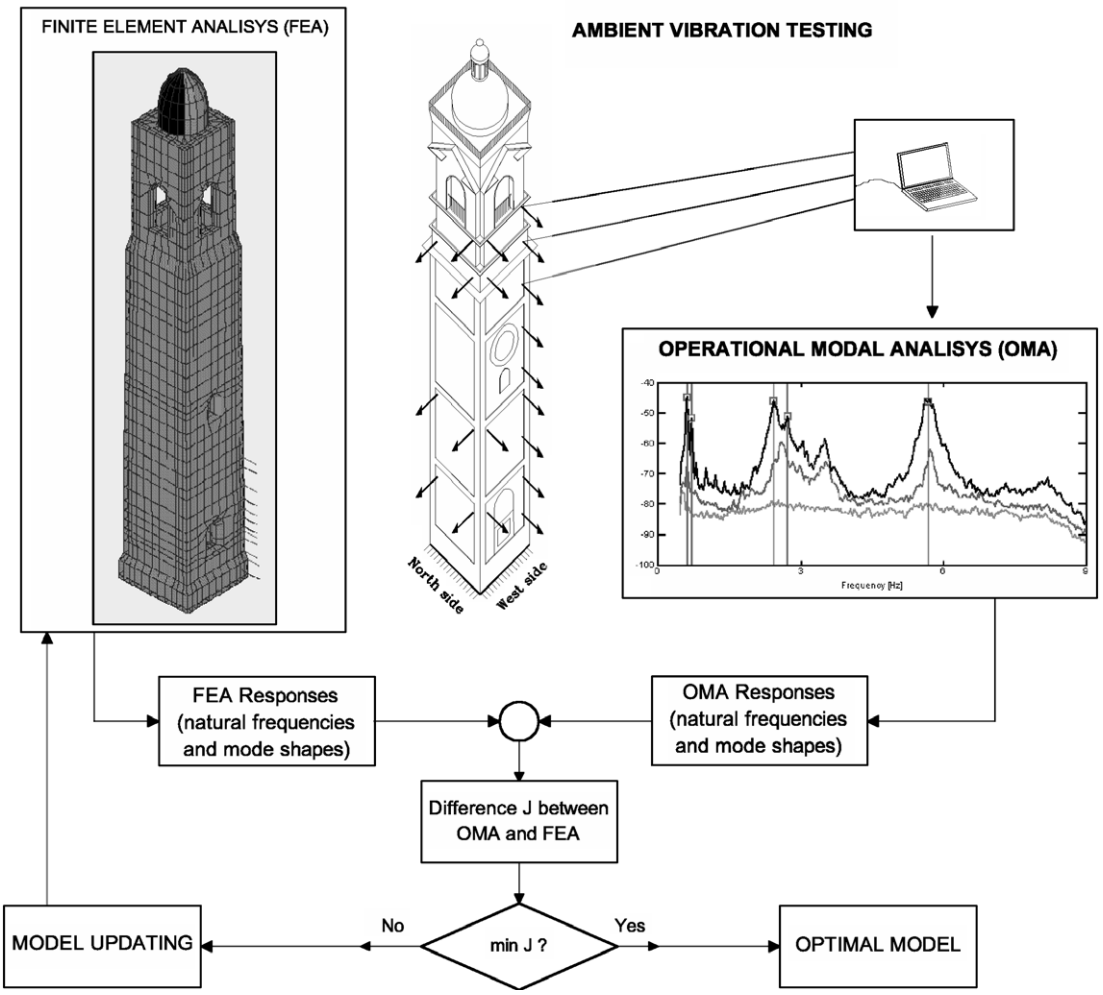

Fig. 1. Dynamic-based assessment of a structure.

ence of major cracks, especially on the western and eastern load-bearing walls. Ambient vibration survey has been preferred in the present application (and it has generally to be preferred for testing an historic structure) because no excitation equipment is needed since the natural or environmental excitations are always present and hence the test implies a minimum interference with the normal use of the structure. Furthermore, ambient vibration testing has recently become the main experimental method available for assessing the dynamic behaviour of full-scale structures and has demonstrated to be especially suitable for flexible systems, such as suspension bridges [9–11], cable-stayed bridges [12–15] and high-rise buildings [16].

The *OMA*, based on output-only measured data, has been carried out in the frequency domain using the classical *Peak Picking* spectral technique [17] and the more recent *Frequency Domain Decomposition* procedure [18].

In the theoretical part of the study, a 3D finite element model, based on the geometric survey of the building, was developed and the main assumptions adopted in the model were first assessed through rough comparison between the results of the *FEA* and the *OMA*. Successively, some uncertain parameters of the model (basically the Young's modulus of the masonry in different regions of the structure) were selected as "updating parameters" and iteratively modified to minimize the differences in the natural frequencies between *FEA* and *OMA*. The application of two well-known system identification techniques, the Inverse Eigensensitivity [6,19] and the Douglas–Reid [20] methods yielded to very similar results. In addition, the optimal models exhibit good agreement in both frequencies and mode shapes for all identified modes, provided that relatively low stiffness ratios were used in the regions of the tower where the major damage has been observed.

Since the tower is currently subjected to a repair intervention [21], a long term goal of this research is to repeat the dynamic tests after the strengthening [13] in order to investigate the correlation between the repair and the changes in the modal parameters of the structure.

2. The bell-tower of the Monza's Cathedral

2.1. Damage description

The bell-tower of the Monza's Cathedral (Fig. 2) was built between 1592 and 1605, probably according to the

Fig. 2. View of Cathedral of Monza and of the investigated bell-tower.

design of Pellegrino Tibaldi. Since the erection required only 14 years, a great uniformity of materials and construction techniques characterises the tower.

The load-bearing walls of the tower, 74 m high and 1.40 m thick, were made of solid masonry bricks and exhibited large, passing-through and potentially dangerous vertical cracks especially on the West and East sides (Fig. 3). These cracks were certainly present before 1927 (when a rough monitoring of the cracks started) and are slowly but continuously opening. In addition, other widespread, vertical and very thin cracks can be observed mainly on the inner faces of the bearing walls; these further cracks are widespread along the four sides of the tower and deeper at the sides of the entrance were the stresses are more concentrated. The observed crack pattern is present up to the height of about 23.0 m. Since the cracks have developed slowly along the years, a possible time dependent behaviour of the material can be supposed due to the heavy dead load, coupled to temperature variations and wind actions [2].

2.2. On-site investigations

Since 1995, an extensive experimental program of field and laboratory tests on cored samples has been carried

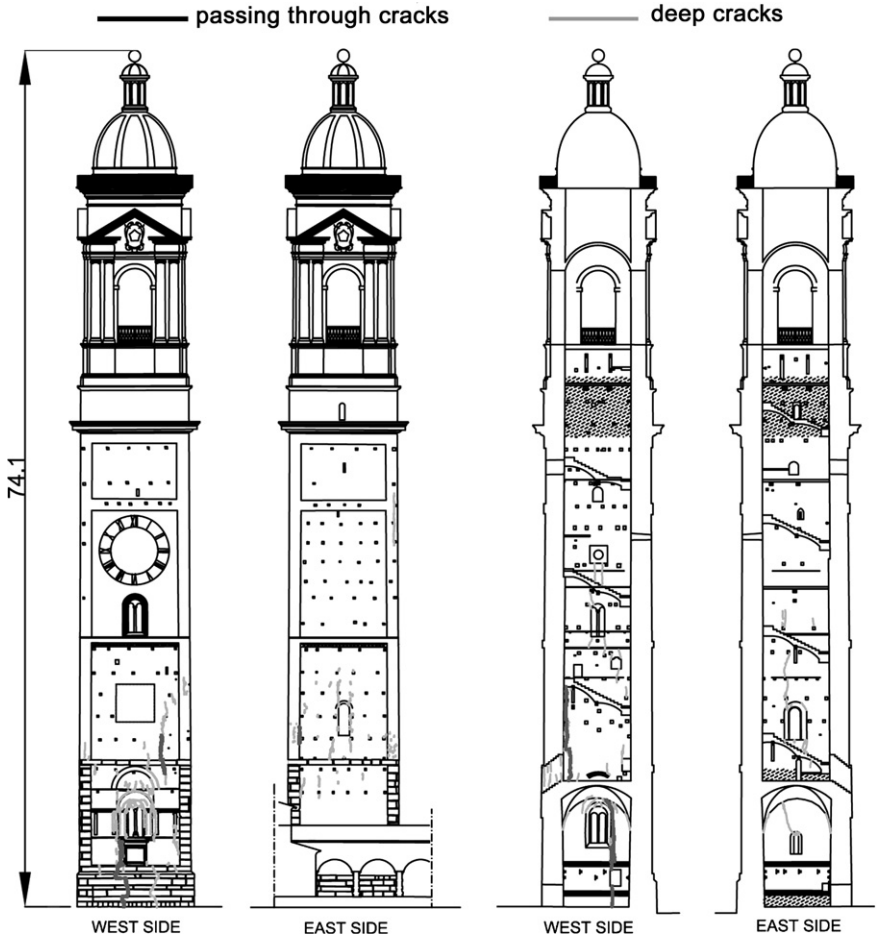

Fig. 3. Crack pattern on the western and eastern walls of the tower (dimensions in m).

out to assess the structural condition of the tower. The complete results of the investigation are reported in [7,8].

First, an accurate field survey of the building configuration was carried out and included the survey of the crack patterns; the cracks were surveyed visually and photographically and reported on plans, prospects and sections. Successively, flat-jack tests were performed in selected points to directly estimate the stress level caused by the dead load. Some double flat-jack tests were also carried out to check the stress–strain behaviour of the masonry under compression; specifically, the Young's modulus was generally ranging between 985 and 1380 N/mm^2 while a Poisson ratio of 0.07–0.20 was detected.

Furthermore, a first series of dynamic tests using four servo-accelerometers was carried out in 1995 to evaluate the natural frequencies of the tower and a structural model was developed, based on the results of the test on the materials [7].

3. Ambient vibration testing

Ambient vibration tests were conducted on the tower at the beginning of July 2001 to measure the dynamic response in 20 different points, with the excitation being associated to environmental loads and to the bell ringing. It is to be noticed that free swinging of the bells was not allowed during the tests because of the presence of temporary scaffolding needed for the repair intervention; in such instances, the bell ringing did not produce any appreciable increase of the vibration level associated with micro-tremors and other ambient excitations.

Fig. 4 shows a schematic representation of the sensor layout; since a maximum of 11 channels was available for the testing and two sensors (placed at points W10, W11 in Fig. 4) were held stationary for reference measurements, a series of two set-ups was required to cover the 20 measurement points of Fig. 4.

The test were conducted using a 16 channel data acquisition system with uniaxial WR-731A piezoelectric sensors (Fig. 5); these sensors allowed acceleration or velocity responses to be recorded. Due to the low level of ambient excitation that existed during the tests, the maximum recorded velocity ranges up to about 0.15 mm/s.

Two-conductor cables connected the accelerometers to a computer workstation with a data acquisition board for A/D and D/A conversion of the transducer signals and storage of digital data. For each channel, the ambient time histories, in terms of both acceleration and velocity, were recorded for 2280 s at intervals of 0.005 s, which resulted in a total of 456,000 data points. Signals converted to digital form were stored on the hard disk of the data acquisition computer in ASCII form.

4. Data processing and operational modal analysis

The extraction of modal parameters from ambient vibration data was carried out by using two different output-only

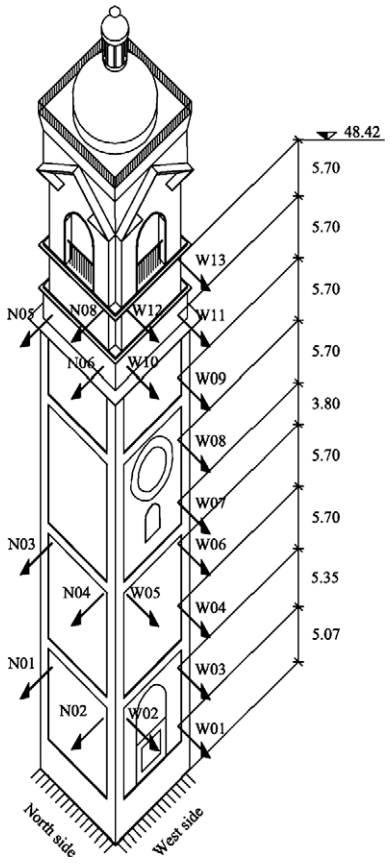

Fig. 4. Sensor locations and directions for the tower test (dimensions in m).

Fig. 5. WR-731 A accelerometer.

procedures: the *Peak Picking* method (*PP*) [17] and the *Frequency Domain Decomposition* (*FDD*) [18]. Both methods are based on the evaluation of the spectral matrix (i.e. the matrix of cross-spectral densities) in the frequency domain

$$\boldsymbol{G}(f) = E[\boldsymbol{A}(f)\boldsymbol{A}^H(f)], \quad (1)$$

where the vector $\boldsymbol{A}(f)$ collects the acceleration responses in the frequency domain, superscript^H denotes complex con-

jugate transpose matrix and E denotes expected value. The diagonal terms of the matrix $\boldsymbol{G}(f)$ are the (real valued) auto-spectral densities (ASD) while the other terms are the (complex) cross-spectral densities (CSD)

$$G_{pp}(f) = E[A_p(f)A_p^*(f)], \tag{2a}$$

$$G_{pq}(f) = E[A_p(f)A_q^*(f)], \tag{2b}$$

where the superscript * denotes complex conjugate.

The ASDs and CSDs were estimated from the recorded time-histories using the modified periodogram method [22]; according to this approach an average is made over each recorded signal, divided into M frames of $2n$ samples, where windowing and overlapping is applied. In the present application, each data record was divided into 8192 points, Hanning-windowed periodograms with 50% overlapping for spectral averaging. The averaging was done using 110 periodograms; since $\Delta t = 0.005$ s, the resulting frequency resolution is $1/(8192 \times 0.005) \approx 0.0244$ Hz.

4.1. Peak picking

The more traditional approach to estimate the modal parameters of a structure [17] is often called *Peak Picking* method. The method leads to reliable results provided that the basic assumptions of low damping and well-separated modes are satisfied. In fact, for a lightly damped structure subjected to a white-noise random excitation, both ASDs and CSDs reach a local maximum at the frequencies corresponding to the system normal modes; hence, in the neighbourhood of a resonant frequency f_r, the spectral matrix can be approximated as

$$\boldsymbol{G}(f_r) \approx \alpha_r \boldsymbol{\phi}_r \boldsymbol{\phi}_r^H, \tag{3}$$

where α_r depends on the damping ratio, the natural frequency, the modal participation factor and the excitation spectra. Eq. (3) highlights that

1. each row or column of the spectral matrix at a resonant frequency f_r can be considered as an estimate of the mode shape $\boldsymbol{\phi}_r$ at that frequency;
2. the square-root of the diagonal terms of the spectral matrix at a resonant frequency f_r can be considered as an estimate of the mode shape $\boldsymbol{\phi}_r$ at that frequency.

In the present application of the PP method, the natural frequencies were identified from resonant peaks in the ASDs and in the amplitude of CSDs, for which the cross-spectral phases are 0 or π. The mode shapes were obtained from the amplitude of square-root ASD curves while CSD phases were used to determine directions of relative motion. For example, the ASDs of the velocity response at selected points of the building are shown in Fig. 6(a); the inspection of the spectral plots generally reveals well defined peaks in the investigated frequency range and a remarkable consistency in their occurrence.

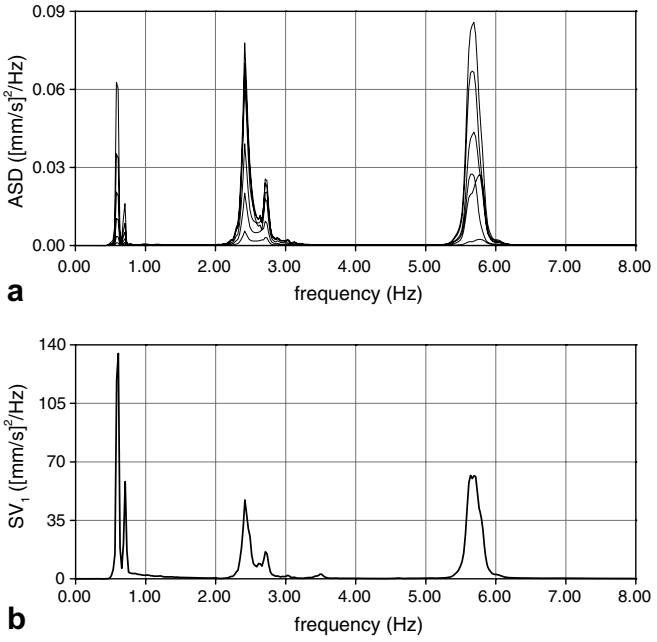

Fig. 6. (a) Autospectra of the velocity response from different points of the tower. (b) First singular value of the (velocity responses) spectral matrix.

Drawbacks of the PP method [9] are related to the difficulties in identifying closely spaced modes and damping ratios.

4.2. Frequency domain decomposition

The FDD technique involved the following main steps: (a) the estimate of the spectral matrix; (b) the Singular Value Decomposition (SVD, see e.g. [23]) of the spectral matrix at each frequency; (c) the inspection of the curves representing the singular values to identify the resonant frequencies and estimate the corresponding mode shape using the information contained in the singular vectors of the SVD.

The SVD of the spectral matrix at each frequency is given by

$$\boldsymbol{G}(f) = \boldsymbol{U}(f)\boldsymbol{\Sigma}(f)\boldsymbol{U}^H(f), \tag{4}$$

where the diagonal matrix $\boldsymbol{\Sigma}$ collects the real positive singular values in descending order and $\boldsymbol{U}$ is a complex matrix containing the singular vectors as columns. The SVD is used for estimating the rank of $\mathbf{G}$ at each frequency, with the number of non-zero singular values being equal to the rank; if only one mode is important at a given frequency f_r (as it has to be expected for well-separated modes) the spectral matrix approximates a rank-one matrix as

$$\boldsymbol{G}(f) \cong \sigma_1(f)\boldsymbol{u}_1(f)\boldsymbol{u}_1^H(f). \tag{5}$$

By comparing Eq. (5) with Eq. (3), it is evident that the first singular vector $\boldsymbol{u}_1(f)$ is an estimate of the mode shape. Since the first singular value $\sigma_1(f)$ at each frequency represents

the strength of the dominating vibration mode at that frequency, the first singular function can be suitably used as a modal indication function (yielding the resonant frequencies as local maxima) as it is shown in Fig. 6(b) for the present application. In addition, the successive singular values contain either noise or modes close to a strong dominating one. The *FDD* is a rather simple procedure that represents an improvement of the *PP* since

1. the *SVD* is an effective method to separate signal space from noise space;
2. the evaluation of mode shapes is automatic and significantly easier than in the *PP*;
3. in case of closely spaced modes around a certain frequency, every singular vector corresponding to a non-negligible singular value represents a mode shape estimate.

4.3. Mode shapes correlation

Once the modal identification phase was completed, the two sets of mode shapes resulting from the application of *PP* and *FDD* were compared by using the well-known Modal Assurance Criterion (*MAC*) [24]. The *MAC* is probably the most commonly used procedure to correlate two sets of mode shape vectors and is defined as follows:

$$MAC(\boldsymbol{\phi}_{A,k}, \boldsymbol{\phi}_{B,j}) = \frac{(\boldsymbol{\phi}_{A,k}^{\mathrm{T}} \boldsymbol{\phi}_{B,j})^2}{(\boldsymbol{\phi}_{A,k}^{\mathrm{T}} \boldsymbol{\phi}_{A,k})(\boldsymbol{\phi}_{B,j}^{\mathrm{T}} \boldsymbol{\phi}_{B,j})}, \tag{6}$$

where $\boldsymbol{\phi}_{A,k}$ is the kth mode of data set A and $\boldsymbol{\phi}_{B,j}$ the jth mode of the data set B. The *MAC* is a coefficient analogous to the correlation coefficient in statistics and ranges from 0 to 1; a value of 1 implies perfect correlation of the two mode shape vectors while a value close to 0 indicates uncorrelated (orthogonal) vectors. In general, a *MAC* value greater than 0.80 is considered a good match while a *MAC* value less than 0.40 is considered a poor match. The *MAC* was also used to correlate the results of *FEA* and *OMA*.

5. Modal behaviour of the tower

Due to the low level of ambient vibrations that existed during the tests, the use of the velocity responses in the *OMA* provided better mode shapes estimates, especially for the lower vibration modes. A total of five vibration modes were identified from ambient vibration data in the frequency range of 0–8 Hz.

The results of the *PP* technique in terms of natural frequencies can be demonstrated through the spectral plots of Fig. 6(a), showing the (velocity) *ASD*s from different locations of the tower. Fig. 6(a) clearly reveals resonant peaks at 0.59, 0.71, 2.46, 2.73 and 5.71 Hz; furthermore, the inspection of the spectral plots in Fig. 6(a) highlights a good consistency of occurrence of spectral peaks; this information and the coherence values [17], which were generally close to one in the frequency range where spectral peaks occur, suggest both a good quality of data and the linearity of the dynamic response. It is worth noting that near unit values of coherence were generally detected in all measurement points for the 1st, 2nd and 5th mode while for the other modes, especially in the lower measurement points, the coherence values suggest a worse signal-to-noise ratio.

As previously said, in the *FDD* procedure the modal frequencies can be located by the peaks of the first singular value of the spectral matrix, as it is shown in Fig. 6(b). The results of *PP* and *FDD* techniques are very similar, with the correspondence in terms of resonant frequencies being particularly evident, since the peaks in Fig. 6(a) and (b) are placed practically at the same frequencies. Furthermore, Table 1 compares the corresponding mode shapes and scaled modal vectors obtained from the two different identification procedures through the frequency discrepancy $D_F = |(f_{PP} - f_{FDD})/f_{PP}|$ and the *MAC*. Inspection of the correlation values summarized in Table 1 highlights a very good agreement between the two methods in terms of both natural frequencies (with the maximum differences not exceeding 2.05%) and mode shapes (with minimum *MAC* value of about 0.96).

Table 1 also summarises the classification of the identified mode shapes. It should be noticed that

1. the classification of mode shapes is based on the availability of sensors up to the height of 48.0 m;
2. the identified frequencies are practically equal to those estimated in the 1995 field test;
3. notwithstanding the nearly symmetric shape of the Tower, the dominant bending modes of the system generally show coupled motion in the two main E–W and N–S directions. Thus, the experimental modal analysis suggests either a strong coupling between the tower and the Cathedral or a non-symmetric stiffness distribu-

Table 1
Modal parameters identified from ambient vibration tests

Mode no.	Mode type	f_{PP} (Hz)	f_{FDD} (Hz)	D_F (%)	*MAC*
1	Bending mode in E–W/N–S direction	0.586	0.598	2.05	0.9984
2	Bending mode in N–S/E–W direction	0.708	0.708	0.00	0.9989
3	Torsion mode	2.456	2.417	1.59	0.9929
4	Bending mode in E–W/N–S direction	2.731	2.722	0.33	0.9597
5	Bending mode in E–W/N–S direction	5.706	5.713	0.12	0.9923

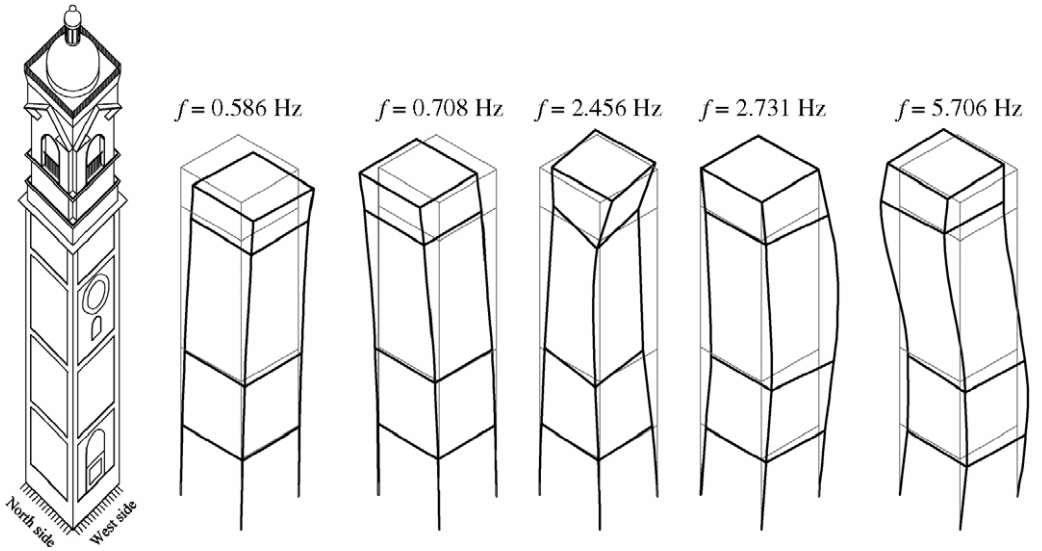

Fig. 7. Vibration modes identified from ambient vibration measurements (*PP*).

tion (as the one which has to be expected basing on the crack distribution). These hypotheses were successively investigated by using a 3D finite element model.

Finally, the experimentally determined modes of the bell-tower are shown in Fig. 7.

6. F.E. modelling and structural identification

6.1. Finite element model

The experimental investigation was preceded by the development of a 3D finite element model (Fig. 8), based on the geometric survey. The tower was modelled using 8-node brick elements while the dome was represented by 4-node shell elements. A relatively large number of finite elements have been used in the model, so that a regular distribution of masses could be obtained and all the main openings in the load-bearing walls could be reasonably represented. The model results in a total of 4944 nodes, 3387 solid elements and 80 shell elements with 14,286 active degrees of freedom. A three-dimensional view of the model is shown in Fig. 8.

In formulating the model, the following assumptions were adopted:

a. the tower footing was considered as fixed;
b. a constant weight per unit volume (18.0 kN/m^3) of the masonry was assumed;
c. the Poisson's ratio of the masonry was held constant and equal to 0.15;
d. the connection between the southern wall of the bell-tower and the facade of the Cathedral was accounted for by introducing rigid constraints in the N–S direction; in the orthogonal E–W direction, the interaction between the tower and the Cathedral was simulated by an uniform distribution of linear elastic springs of constant k (Fig. 8).

The structural parameters of the tower affected by major uncertainties are obviously related to the distribution of the Young's modulus in the masonry and to the spring constant k. The range of variation (i.e. the upper and lower bounds) of these parameters was estimated accounting

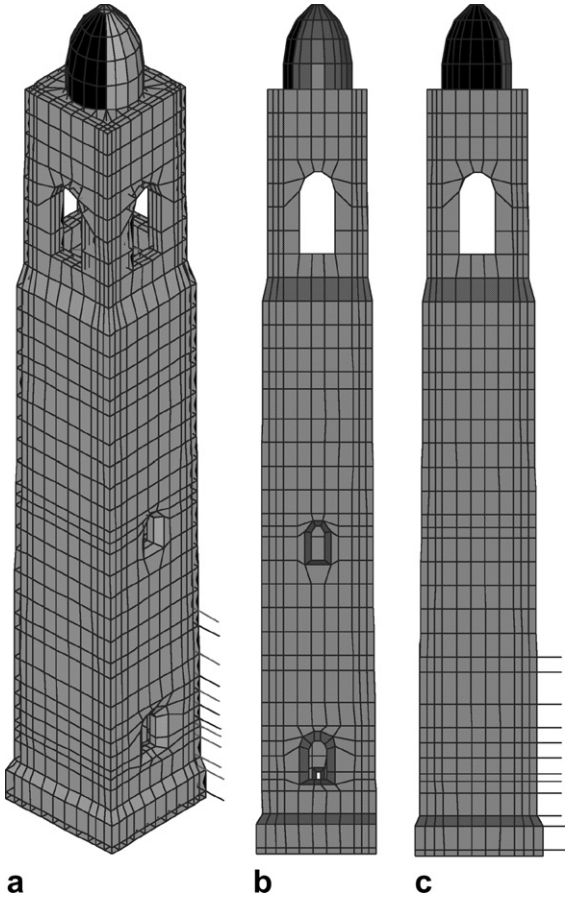

Fig. 8. Finite element model of the bell-tower: (a) 3D view; (b) West side; (c) North-side.

for the results of the masonry characterization and to ensure a broad correspondence between theoretical and experimental modal characteristics.

In order to approximately represent the damaged areas of the tower, a non-homogeneous distribution of the Young's modulus was assumed. To limit the number of structural parameters in the structural identification procedure, the building was divided in six regions, with the masonry Young's modulus being assumed as constant within each zone. Since the major cracks were placed along the East- and West-sides of the tower up to about 20.0–23.0 m, the lower part of the tower ($h \leqslant 23.0$ m) was divided into five sub-regions by distinguishing the four load-bearing walls and the corner properties, as it is shown in Fig. 9. In addition, the updating included two further parameters: the average elastic modulus in the upper part of the tower and the spring constant k.

Hence, the finite element model updating was carried out with respect to the set of seven structural parameters summarised in Table 2

1. the Young's moduli E_i ($i = 1,2,\ldots,5$) in the lower part of the tower (Fig. 9);
2. the Young's modulus E_6 in the upper part of the tower;
3. the elastic constants k of the springs placed along the contact area between the Cathedral and the bell-tower in the direction of the Southern wall;

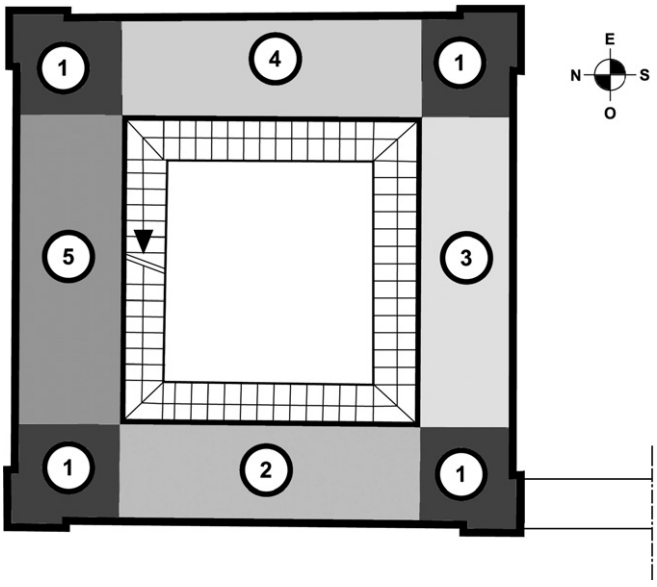

Fig. 9. Regions selected for the Young's modulus identification (height $\leqslant$ 23.0 m).

6.2. Structural identification procedures

The uncertain structural parameters were estimated by minimizing the difference between theoretical and experimental natural frequencies. Specifically, two different well-known system identification algorithms were used: the Inverse Eigen-Sensitivity (*IE*) [6,19] and the Douglas–Reid (*DR*) [20] methods, with both techniques requiring the estimate of upper and lower bounds of the updating parameters.

In the *IE* technique, the functional relationship between the measured responses and the structural parameters X of the model is expressed in terms of a Taylor series expansion limited to the linear terms as

$$\boldsymbol{R}_e = \boldsymbol{R}(\boldsymbol{X}_o) + \boldsymbol{S}(\boldsymbol{X} - \boldsymbol{X}_o), \tag{7}$$

where $\boldsymbol{R}_e$ is the vector associated with the reference response test data, $\boldsymbol{R}(\boldsymbol{X}_o)$ is a vector containing the responses from the model corresponding to the starting choice $\boldsymbol{X}_o$ of the updating parameters and $\boldsymbol{S}$ is the sensitivity matrix, with terms $\partial R_i/\partial X_k$. Eq. (7) is then used to derive the following iteration scheme to evaluate $\boldsymbol{X}$:

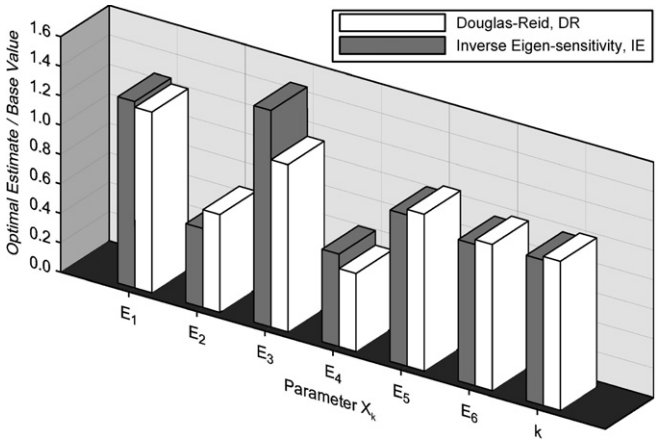

Fig. 10. Optimal estimates of the structural parameters.

Table 2
Structural parameters of the updated models

Structural parameter	Lower value	Base value	Upper value	Updated model	
				DR	*IE*
E_1 (N/mm^2) Corner (height $\leqslant$23 m)	800	1400	2500	1718	1772
E_2 (N/mm^2) West wall (height $\leqslant$23 m)	500	1400	1800	930	751
E_3 (N/mm^2) South wall (height $\leqslant$23 m)	800	1400	2500	1591	2060
E_4 (N/mm^2) East wall (height $\leqslant$23 m)	500	1400	1800	742	880
E_5 (N/mm^2) North wall (height $\leqslant$23 m)	800	1400	2500	1493	1440
E_6 (N/mm^2) All walls (height $\geqslant$23 m)	800	1400	1800	1789	1729
k (kN/m^3)	34,450	68,900	86,250	69,730	67,987

$$\boldsymbol{X}_{n+1} = \boldsymbol{X}_n + \boldsymbol{H}[\boldsymbol{R}_e - \boldsymbol{R}(\boldsymbol{X}_n)], \tag{8}$$

where the gain matrix $\boldsymbol{H}$ is generally computed either using the Moore–Penrose pseudo-inverse ($\boldsymbol{H} = \boldsymbol{S}^T(\boldsymbol{S}\boldsymbol{S}^T)^{-1}$) or following the Bayesian estimation theory [6,19].

According to the *DR* approach [20], the relationship between any response (natural frequencies and mode shapes) of the model and the structural parameters X_k ($k = 1,2,\ldots,N$) of the model is approximated around the current values of X_k by the following:

$$R_i^*(X_1, X_2, \ldots, X_N) = \sum_{k=1}^{N} [A_{ik} X_k + B_{ik} X_k^2] + C_i, \tag{9}$$

where R_i^* represents the approximation of the ith response of the finite element model.

Eq. (9) clearly shows that $(2N+1)$ coefficients A_{ik}, B_{ik} and C_i must be determined before to compare each R_i^* to its experimental counterpart in a system identification algorithm. In order to evaluate these constants, engineering judgement is first used to estimate a base value of the structural parameters $X_k^B (k = 1, 2, \ldots, N)$ and the range in which such variables can vary. Let us denote the lower and upper limits of the unknown parameters as X_k^L and $X_k^U (k = 1, 2, \ldots, N)$, respectively

$$X_k^L \leqslant X_k \leqslant X_k^U.$$

Then, the $(2N+1)$ constants on the right hand side of Eq. (9) are determined by computing the ith response R_i^{FEM} of the finite element model for $(2N+1)$ choices of the unknown parameters. The first choice of the structural parameters corresponds to the base values; then each structural unknown is varied, one at time, from the base value to the upper and lower limit, respectively. Thus, the $(2N+1)$ conditions used to evaluate the constants in Eq. (9) are the following:

$$\begin{aligned}
&R_i^*(X_1^B, X_2^B, \ldots, X_N^B) = R_i^{\mathrm{FEM}}(X_1^B, X_2^B, \ldots, X_N^B)\\
&R_i^*(X_1^L, X_2^B, \ldots, X_N^B) = R_i^{\mathrm{FEM}}(X_1^L, X_2^B, \ldots, X_N^B)\\
&R_i^*(X_1^U, X_2^B, \ldots, X_N^B) = R_i^{\mathrm{FEM}}(X_1^U, X_2^B, \ldots, X_N^B)\\
&\cdots\\
&R_i^*(X_1^B, X_2^B, \ldots, X_N^L) = R_i^{\mathrm{FEM}}(X_1^B, X_2^B, \ldots, X_N^L)\\
&R_i^*(X_1^B, X_2^B, \ldots, X_N^U) = R_i^{\mathrm{FEM}}(X_1^B, X_2^B, \ldots, X_N^U)
\end{aligned} \tag{10}$$

Once the coefficients A_{ik}, B_{ik} and C_i have been computed, the approximation (9) is completely defined and it can be used to update the structural parameters. The optimal parameter estimates are defined to be the values which minimise the following:

$$\begin{aligned}
&J = \sum_{i=1}^{M} w_i \varepsilon_i^2\\
&\varepsilon_i = R_i - R_i^*(X_1, X_2, \ldots, X_N)
\end{aligned} \tag{11}$$

where R_i represents the ith experimental response and w_i is a weighting constant.

6.3. Comparison with the experimental results

Table 2 lists the optimal estimates of the structural parameters obtained from *DR* and *IE* methods, the base values and the assumed lower and upper limits; furthermore, Fig. 10 shows the optimal estimates normalized with respect to their initial values. By examining Table 2 and Fig. 10, the following comments can be made:

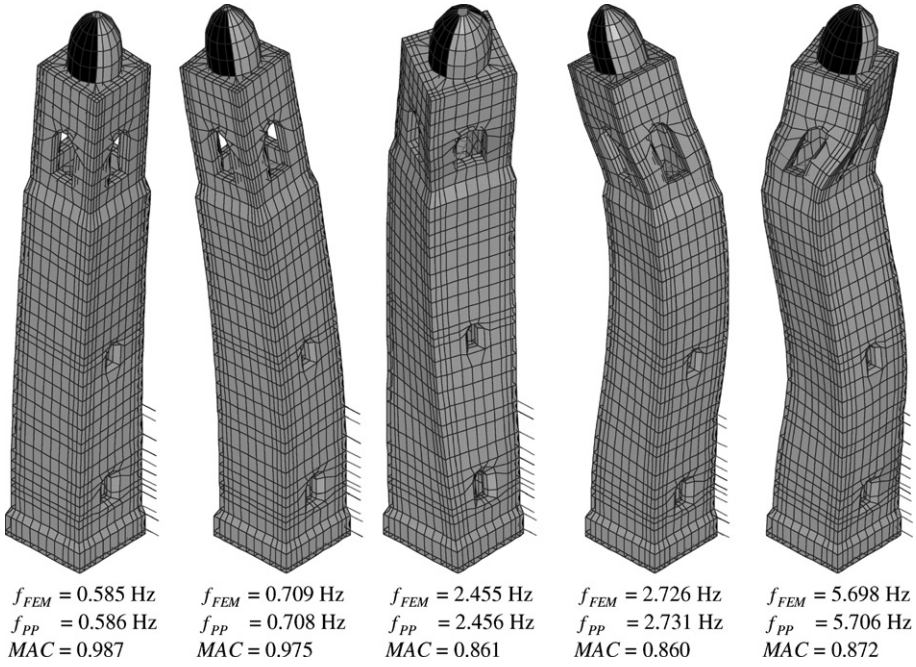

Fig. 11. Vibration modes of the updated model (*DR* method) and comparison with the experimental results.

1. the two sets of identified parameters provide coherent information on the stiffness distribution. The optimal estimates obtained from the two techniques, although numerically different, are generally in close agreement. This correspondence provides an important indication on the reliability of the numerical estimates;
2. the main difference between the optimal estimates is related to the elastic modulus E_3 of the Southern wall, probably as a consequence of the minor sensitivity of E_3 to the changes of the response parameters;
3. both the sets of estimated parameters seem to represent very well the damage distribution of the tower and are also in good agreement with the double flat-jack results. Specifically, a low stiffness ratio is detected for the Eastern and Western load-bearing walls up 23.0 m, with the Young's modulus in such regions being about the half of the values obtained in the other parts of the tower;
4. in the lower part of the tower, the Young's modulus turns out to be higher in the corner zones than elsewhere. This result is fully consistent with the traditional construction techniques, generally characterised by the adoption of the best available materials and skills in the corners.

Fig. 11 shows the vibration modes of the *DR* updated model, corresponding to the experimental ones, and the correlation with the experimental modal behaviour. The natural frequencies of the *DR* optimal model are practically equal to the experimental ones, as it has to be expected since the identification procedure was based on the minimisation of the frequency discrepancies. The correlation between mode shapes shows very good agreement with the experimental results for the first two modes (with the *MAC* being greater than 0.97); for the higher modes, the *MAC* is in the range 0.86–0.87 so that appreciable average differences are detected. Such differences are probably to be related either to the simplified distribution of the model elastic properties (which were held constant for large zones of the structure) or to a relative lack of accuracy in the experimental evaluation of the higher mode shapes. A similar correlation was found for *IE* updated model as well.

7. Conclusions

Theoretical and experimental dynamic investigation of a historic masonry bell-tower is described in the paper. The following conclusions can be drawn from the study:

1. Within the frequency range 0–10 Hz, five vibration modes were clearly identified.
2. The measurement of structural response to the ambient levels of vibration has proved to be an effective means for the identification of the dynamic properties of masonry towers, although in some measurement points the signal-to-noise ratio turned out to be quite low.
3. A very good agreement was found between the modal estimates obtained from the *Peak Picking* [17] and the *Frequency Domain Decomposition* [18] techniques.
4. The fundamental mode of the bell-tower, with a natural frequency of about 0.59 Hz, involves dominant bending in the E–W direction with significant bending participation in the opposite N–S direction as well; the coupled motion in the two main E–W and N–S directions characterizes all the tower mode shapes.
5. The comparison between measured and predicted modal parameters was used to verify the assumptions adopted in formulating the model. Specifically, a good match between theoretical and experimental modal parameters was reached for relatively low values of the model Young's modulus in the most damaged regions of the tower. Furthermore, the dynamic-based model updating, carried out by using two different methods, led to consistent structural parameters (distribution of Young's modulus in the masonry) which are in close agreement with the results of double flat-jack tests.
6. Due to the good correlation between experimental and theoretical modal behaviour, the updated models seem to be adequate to provide reliable predictions under the load conditions interesting to assess the structural safety of the tower.
7. The dynamic-based assessment of masonry towers seems a promising approach to evaluate damage in such structures provided that an accurate geometric survey is available and in the hypothesis that the damage scenario mainly involves the lower regions of the building, where high eigen-sensitivity has to be expected.

Acknowledgements

The research was supported by the Italian Ministry of University and Research (M.I.U.R.).

The authors are indebted with Prof. L. Binda and Prof. C. Modena, for having allowed and encouraged the research.

Dr. N. Gallino is gratefully acknowledged for the help in developing the application of *IE* identification procedure; M. Antico, L. Cantini and M. Cucchi are acknowledged for the assistance in conducting the field tests.

References

[1] Binda L, Gatti G, Mangano G, Poggi C, Sacchi Landriani G. The collapse of the Civic Tower of Pavia: a survey of the materials and structure. Masonry Int 1992;20(6):11–20.

[2] Binda L, Anzani A, Mirabella Roberti G. The failure of ancient Towers: problems for their safety assessment. In: Proceedings of the 4th International Conference on Structural Studies, Repairs and Maintenance of Heritage Architecture, STREMAH 95, Crete: Chania, 1995. p. 179–186.

[3] Binda L, Tongini Folli R, Mirabella Roberti G. Survey and investigations for the diagnosis of damage in masonry structures: the "Torrazzo" of Cremona. In: Proceedings of the 12th International brick/block Masonry conference, Madrid, Spain, 2000. p. 237–257.

[4] Valluzzi MR, da Porto F, Modena C. Structural investigation and strengthening of the Civic Tower in Vicenza. In: Proceedings of Structural Faults and Repairs 2003, UK: London, 2003 (10 pages, on CD-ROM).
[5] Lionello A, Cavaggioni I, Modena C, Casarin F, Rossi PP, Rossi C. Experimental and numerical analysis of the structural behaviour of St. Stefano's bell-tower in Venice. In: Proceedings of the 4th International seminar on structural analysis of Historic Constructions, Italy: Padova, 2004. p. 533–542.
[6] Friswell MI, Mottershead JE. Finite element model updating in structural dynamics. The Netherlands, Dordrecht: Kluwer Academic; 1995.
[7] Binda L, Poggi C. Assessment of the mechanical behaviour of materials and structures of the bell-tower adjacent to the Cathedral of Monza by on-site tests and numerical simulation. Technical Report, Politecnico di Milano, 1997 [in Italian].
[8] Binda L, Tiraboschi C, Tongini Folli R. On site and laboratory investigation on materials and structure of a bell-tower in Monza Int. Zeitschrift für Bauinstandsetzen und baudenkmalpflege 2000;6(1): 41–62.
[9] Abdel-Ghaffar AM, Housner GW. Ambient vibration tests of suspension bridge. J Engineering Mechanics Div ASCE 1978;104(5):983–99.
[10] Abdel-Ghaffar AM, Scanlan RH. Ambient vibration studies of Golden Gate bridge. I: Suspended structure. J Eng Mech Div ASCE 1985;111(4):463–82.
[11] Brownjohn JMW, Dumanoglu AA, Severn RT. Ambient vibration survey of the Faith Sultan Mehmet (Second Bosporus) suspension bridge. Earthquake Eng Struct Dynam 1992;21: 907–24.
[12] Wilson JC, Liu T. Ambient vibration measurements on a cable-stayed bridge. Earthquake Eng Struct Dynam 1991;20:723–47.
[13] Gentile C, Martinez y Cabrera F. Dynamic investigation of a repaired cable-stayed bridge. Earthquake Eng Struct Dynam 1997;26:41–59.
[14] Brownjohn JMW, Xia PQ. Dynamic assessment of curved cable-stayed bridge by model updating. J Struct Eng ASCE 2000;126(2):252–60.
[15] Gentile C, Martinez y Cabrera F. Dynamic performance of twin curved cable-stayed bridges. Earthquake Eng Struct Dynam 2004;33: 15–34.
[16] Brownjohn JMW. Ambient vibration studies for system identification of a tall building. Earthquake Eng Struct Dynam 2003;32:71–95.
[17] Bendat JS, Piersol AG. Engineering applications of correlation and spectral analysis. 2nd ed. USA, New York: Wiley Interscience; 1993.
[18] Brincker R, Zhang LM, Andersen P. Modal identification from ambient responses using Frequency Domain Decomposition. In: Proceedings of the 18th International Modal Analysis Conf., USA: San Antonio, 2000.
[19] Collins JD, Hart GC, Hasselmann TK. Statistical identification of structures. AIAA J 1974;12(2):185–90.
[20] Douglas BM, Reid WH. Dynamic tests and system identification of bridges. J Struct Div ASCE 1982;108(10):2295–312.
[21] Modena C, Valluzzi MR, Tongini Folli R, Binda L. Design choices and intervention techniques for repair and strengthening of the Monza Cathedral bell-tower. In: Proceeding of the Structural Faults and Repairs 2001, UK: London, 2001 (12 pages, on CD-ROM).
[22] Welch PD. The use of Fast Fourier Transform for the estimation of Power Spectra: a method based on time averaging over short modified periodograms. IEEE Trans 1967;AU-15:70–73.
[23] Golub GH, Van Loan CF. Matrix Computations. 3rd ed. J. Hopkins University Press; 1996.
[24] Allemang RJ, Brown DL. A correlation coefficient for modal vector analysis. In: Proceedings of the 1st International Modal Analysis Conference, USA: Orlando, 1982. p. 110–116.